Plant Physiology and Biochemistry 142 (2019) 460–471

Contents lists available at ScienceDirect

Plant Physiology and Biochemistry

journal homepage: www.elsevier.com/locate/plaphy

Research article

Phyllanthus emblica fruit extract stabilized biogenic silver nanoparticles as a growth promoter of wheat varieties by reducing ROS toxicity

Rekha Kannaujia[a,c], Chandra Mohan Srivastava[b], Vivek Prasad[c], Brahma N. Singh[d], Vivek Pandey[a,*]

[a] Plant Ecology and Climate Change Science, CSIR-National Botanical Research Institute, Rana Pratap Marg, Lucknow, 226001, U.P, India
[b] Centre for Polymer Technology, Amity School of Applied Sciences, Amity University Haryana, Gurgaon, 122413, India
[c] Molecular Plant Virology Lab, Department of Botany, University of Lucknow, Lucknow, 226007, U.P, India
[d] Pharmacognosy & Ethnopharmacology Division, CSIR-National Botanical Research Institute, Rana Pratap Marg, Lucknow, 226001, U.P, India

ARTICLE INFO

Keywords:
Silver nanoparticles
Phyllanthus emblica L.
Antioxidant activity
Reactive oxygen species
Wheat

ABSTRACT

The present study is focused on the biogenic synthesis of AgNPs (B-AgNPs) using fruit extract of *Phyllanthus emblica* L. and its effect (0, 5, 10, 25, 50 mg/L concentrations) on early seedling growth of two wheat varieties (HD-2967 and DBW-17). The prepared silver nanoparticles were characterized with several techniques such as UV–Vis spectroscopy, powder X-ray diffraction as well as high-resolution transmission electron microscopy. The capping of AgNPs by phytochemicals was confirmed by Fourier transforms infrared (FT-IR) spectroscopy. B-AgNPs, chemically synthesized AgNPs, chemically synthesized AgNPs + 10% fruit extract and $AgNO_3$ salt were compared for phytotoxicity, based on growth parameters, ROS production, cytotoxicity assay and silver accumulation in two wheat varieties (HD-2967 and DBW-17). These effects were more pronounced in the variety HD-2967 over DBW-17 variety at 10 mg/L B-AgNPs exposure. Root cells viability of treated radicles was studied using Evans blue dye assay which suggest that 10 mg/L B-AgNPs was effective in promoting early seedling growth by decreasing ROS toxicity. Lower accumulation of Ag resulting in higher root cell viability than those of chemically synthesized AgNPs treated seedlings. The findings of the present study clearly indicate that phytochemicals capped AgNPs act as a growth promoter at lower concentrations by delivering a potent antioxidant during early seedling growth as compared to chemically synthesized AgNPs treated wheat seedlings.

1. Introduction

Seed germination and early seedling development are two important phases of crop plants for sustainable agriculture. During seed germination, many biochemical and cellular events trigger the production of reactive oxygen species (ROS) (Wojtyla et al., 2016). The reactive oxygen species such as superoxide radical ($O_2^{\cdot-}$), hydroxyl radical ($^{\cdot}OH$), hydrogen peroxide (H_2O_2), and singlet oxygen ($^1O_2$) are byproducts of many biochemical processes in plants (Sharma et al., 2012). Low levels of ROS are produced in seeds after imbibition to break dormancy and initiate seed germination. A negative impact in the absence of an efficient antioxidant observed on seed germination during seedling growth as high ROS level result in oxidative stress (Kumar et al., 2015). ROS as well as different plant hormones such as auxin, cytokinin and ethylene, control seed germination and early seedling growth (He et al., 2012). Among these, ROS are key signaling molecule for breaking the dormancy in a concentration-dependent manner. Studies on *Oryza sativa* and *Arabidopsis thaliana* have shown that suppression of ROS generation inhibited seed germination (Leymarie et al., 2012). The role of ROS are crucial since low ROS generation can break seed dormancy, while abundant levels can inhibit seed germination as well as seedling growth (Bailly et al., 2008). Therefore, plants have an efficient antioxidant system to fine tune ROS levels for better seedling growth. Exogenous application of antioxidants such as ascorbic acid (ASA) promotes seed germination and seedling growth even under saline stress (Shalata and Neumann, 2001; Wang et al., 2019).

Abbreviations: AgNPs, Silver nanoparticles; B-AgNPs, Biogenic AgNPs; C-AgNPs, Chemically synthesized AgNPs; C-AgNPs + 10% FE, Chemically synthesized AgNPs + 10% fruit extract; Control, Without AgNPs treatment (MQ water); $AgNO_3$, Silver nitrate; *Phyllanthus emblica* L., *P. emblica*; ROS, Reactive oxygen species; FE, Fruit Extract; DPPH, 1,1-diphenyl-2-dipicrylhydrazyl; DAT, A Day after treatment; RL, Radicle length; PL, Plumule length; RDW, Radicle dry weight; PDW, Plumule dry weight; SVI, Seedling vigor index; RRE, Relative root elongation; GI, Germination index

* Corresponding author.
E-mail address: v.pandey@nbri.res.in (V. Pandey).

https://doi.org/10.1016/j.plaphy.2019.08.008
Received 29 May 2019; Received in revised form 8 August 2019; Accepted 12 August 2019
Available online 13 August 2019

In recent years, nanotechnology has become a fast-growing area of science, that has potential to enhance agriculture production and be utilized to promote growth and productivity of the plants (Gogos et al., 2012; Walker et al., 2017). Materials synthesized using nano-technology-such as nano-fertilizers, nano-pesticides, nano-sensors to detect pathogens (Chhipa and Joshi, 2016). Nanomaterials based agricultural formulations & devices have been successfully used for controlling and managing plant diseases (Liu and Lal, 2015). In particular, silver nanoparticles (AgNPs) have been used in substantially higher numbers compared to other nanomaterials such as ZnO, TiO_2, and nanosized carbon allotropes (Farkas et al., 2011; McGillicuddy et al., 2017). However, the field of nano-agriculture remains inadequately explored as compared to biomedical and pharmaceutical sciences. Nanomaterials based environmental toxicity is still a point of controversy and debate. Some studies have been carried out to determine the toxic effects of nanoparticles on seed germination (Barrena et al., 2009; Lee et al., 2012). It is reported that AgNPs have significant effects on the growth and yield of crop plants which depend on the surface, size and capping stability (Lu et al., 2010). Limited studies show both positive and negative effects of AgNPs on plants (Nair, 2016; Tripathi et al., 2017). Phytotoxicity in plants depend on the methods of application and duration of exposure as well as on size, concentration, solubility, capping, chemical composition and aggregation of nanoparticles (Nel et al., 2006). Utilization of plant extracts for synthesis of nano-scale metallic particles have received considerable attention over the chemical and physical methods in last decade (Sathishkumar et al., 2009; Zahran et al., 2014).

Nowadays, various plant parts *Erythrina suberosa* leaf extract (Mohanta et al., 2017a), *Phoenix dactylifera* root hair extract (Oves et al., 2018), flower extract of *Malva sylvestris* (Esfanddarani et al., 2017) and seed extract of *Alpinia katsumadai* (He et al., 2017) have been used to synthesize AgNPs. Only few reports are there on synthesis of silver nanoparticles using fruits (Ahmed et al., 2016). Recently, Masum et al. (2019) synthesized AgNPs using *Phyllanthus emblica* fruit extract and explored them as an attractive and eco-friendly candidate to control rice bacterial disease. Other scientists have also synthesized silver nanoparticles using *P. emblica* and reported their antimicrobial property (Ankamwar et al., 2005; Ramesh et al., 2015). However, its phytostimulatory effects on seed germination and seedling growth have not been studied. Thus, the present study aimed to assess (1) environmental benign green synthesis and characterization of B-AgNPs; (2) optimization of the B-AgNPs dose for improved seed germination and seedling growth in two wheat varieties; (3) a comparative study to demonstrate the phytotoxicity of other AgNPs i.e, chemically synthesized AgNPs, chemically synthesized AgNPs + 10% fruit extract and bulk $AgNO_3$ salt and; (4) bioaccumulation of silver content in all AgNPs treated wheat seedlings.

2. Materials and methods

2.1. Materials

Fresh and healthy *Phyllanthus emblica* L. (Hindi-Amla, family Phyllanthaceae) fruits were collected from the garden of CSIR-NBRI, thoroughly washed with deionized Milli-Q (MQ) water and air dried. Two varieties of wheat (*Triticum aestivum* L.) namely var. 'HD-2967' and var. 'DBW-17' were selected for this study. Wheat seeds were purchased from the local market of Lucknow. Silver nitrate and 2,2-diphenyl-1-picrylhydrazyl were purchased from Sigma Aldrich while acetone and ethanol from HiMedia (Mumbai, India). MQ water was used throughout the study. All other chemicals used in this study were purchased from Sigma Aldrich unless specified.

2.2. Preparation of P. emblica fruit extracts (FE)

P. emblica fruit pieces (25 g) were boiled in 100 mL of MQ water for 15 min. After cooling, the extract was filtered through Whatman no.1 filter paper (pore size 25 μm) twice and stored in a refrigerator at 4 °C for further studies. The resultant filtrate was used as reducing and stabilizing agent for silver nanoparticles (AgNPs).

2.3. Synthesis and purification of silver nanoparticles (B-AgNPs)

Silver nanoparticles were synthesized by a green approach as described by Geethalakshmi and Sarada (2010) with slight modifications. Briefly, *P. emblica* fruit extract (10 mL) was added to 100 mL aqueous solution of 1 mM silver nitrate and allowed to react at ambient temperature. The color of reaction mixture changes from transparent yellow to dark brown within 30 min indicating the formation of AgNPs. The solution was centrifuged at 8000 rpm for 15 min. The solid residue was re-dispersed in 50 mL MQ and centrifuged at 5000 rpm for 15 min to isolate the NPs. AgNPs was collected carefully and lyophilized (LABCONCO) for 24 h to obtain the dry powder of AgNPs, which was used for characterization and further studies.

2.4. Characterization of synthesized B-AgNPs

The surface plasmon resonance and spectral analysis of the AgNPs were carried out using UV–Visible spectrophotometer (Agilent Cary 300). The periodic scans of the optical absorbance between 300 and 800 nm were performed to investigate the reduction rate of silver ions by *P. emblica* fruit extract. The reaction mixture was diluted 10 times with MQ before recording the UV-VIS spectra. The size and zeta potential analysis of B-AgNPs were examined by the dynamic light analyzer (DLS) with zeta potential using Malvern Zetasizer Nano range instrument (Malvern Instruments Ltd., Malvern, UK). The surface morphology and size of the synthesized AgNPs were examined by Scanning electron microscope (SEM) and High-resolution transmission electron microscopy (HR-TEM). SEM analysis was performed using the Hitachi S-3700 N SEM at an accelerating voltage of 15 kV. The SEM sample was prepared by making a thin film on a carbon tape and dried under a mercury lamp for 5 min. A drop of the sonicated aqueous suspension of AgNPs was put on carbon-coated copper grid (FEI Technai S Twin) and dried for TEM analysis. This analysis was carried out at 200 kV voltage and 10–30,000× magnification. The elemental analysis was carried out using Energy dispersive X-rays (EDX) attached with SEM. The phase purity and average crystallite size of the synthesized AgNPs were examined by powder X-ray diffractometer (XRD) using monochromatic Cu K_α radiation with a wavelength (λ) of 1.5406 Å and scan rate 0.2 s/step (step size 0.02°), fitted with nickel monochromator at the voltage of 40 kV and tube current of 30 mA (Bruker D8 advance, Germany). The Fourier transform infrared (FT − IR) spectroscopy data was collected on Thermo Scientific Nicolet 380 in the transmission mode between 4000 and 500 cm^{-1} using KBr pallet. The KBr pallets were prepared by grinding the sample with KBr powder in 1:100 ratio.

2.5. Antioxidant activity

2.5.1. DPPH (2, 2-diphenyl-1-picrylhydrazyl) free radical scavenging assay

The free radical scavenging activity of B-AgNPs and *P. emblica* fruit extract (FE) were determined by DPPH assay developed by Choi et al. (2002) with some modifications. Briefly, different concentrations of B-AgNPs and FE (1–50 μg/mL) were mixed with 0.1 mM DPPH methanolic solution in 1:4 ratio. Reaction mixtures (1 mL) were vortexed and incubated in dark for 30 min at 25 °C before measuring absorbance at 517 nm against a blank (methanol) on the microplate reader. The free radical scavenging ability of B-AgNPs and FE was expressed as %inhibition (I) of DPPH which was calculated using the following equation:

$$\%I = \frac{\text{Absorbance of Control} - \text{Absorbance of Sample}}{\text{Absorbance of Control}} \times 100$$

2.6. Phytotoxicity assay

2.6.1. Preparation of different AgNPs suspensions and silver nitrate solutions

Chemically synthesized AgNPs (C-AgNPs) were obtained from Delhi Technological University (DTU), Delhi, India. The size of the obtained C-AgNPs was observed using transmission electron microscopy (Fig. S1). Five different treatments; Control (untreated), B-AgNPs, C-AgNPs, C-AgNPs + 10% FE and silver nitrate salt with four different concentrations (5, 10, 25 and 50 mg/L) were used to determine the phytotoxicity on two wheat varieties. For the phytotoxicity assay, different AgNPs and $AgNO_3$ suspensions were prepared in MQ and sonicated (Q Sonica, 100W, 40 KH_z) for 15 min.

2.6.2. Seed germination experiment

The healthy wheat seeds were sterilized using sodium hypochlorite solution (10% v/v) for 10 min (USEPA, 1996). After sterilization, the seeds were washed with distilled water with vigorous shaking to remove any traces of hypochlorite from seeds. A gentle shaking for 2 h was carried out by putting sterilized seeds of both the varieties in MQ (control), different AgNPs suspensions and $AgNO_3$ solution (5, 10, 25, 50 mg/L) for the determination of seed germination assay. Five seeds from both the wheat varieties were transferred in evenly placed petri dishes (100 mm × 15 mm) having a piece of filter paper (Whatman no. 1) at the bottom. 5 ml of MQ (control), AgNPs, and $AgNO_3$ solutions were added separately to each petri dish. Petri dishes were covered and sealed with parafilm and incubated at 25 °C in dark. All seed germination were observed after 6 days of the treatment. The radicle and plumule length were measured. The Seedling vigor index (SVI) was calculated according to the formula reported by Abdul-Baki and Anderson (1973). The seed germination parameters i.e., percentage of relative root elongation (E) and germination index (GI) were calculated according to the standard methods using Equation (1) − (3) (Tiquia et al., 1996; US Department of Agriculture and US Composting Council, 2001).

$$\text{Relative root elongation (E)} = \frac{\text{(Mean root length with AgNPs)}}{\text{Mean root length with control}} \times 100 \quad (1)$$

$$\text{Germination index (GI)} = \frac{\text{(Relative seed germination)} \times \text{(Relative root elongation)}}{100} \quad (2)$$

$$\text{Relative seed germination} = \frac{\text{(Seed germinated with AgNPs)}}{\text{(Seed germinated with control)}} \times 100 \quad (3)$$

Seedling vigor index (SVI I) = Germination percentage × (Root length + Shoot Length)

Seedling vigor index (SVI II) = Germination percentage × (Root dry weight + Shoot dry weight)

Dose-dependent experiments (0, 5, 10, 25, 50 mg/L) were conducted to assess the effects of B-AgNPs, C-AgNPs, C-AgNPs + 10% FE and $AgNO_3$ on seed germination, and other important seed germination parameters like radicle length (RL), Plumule length (PL), radicle dry wt. (RDW), plumule dry wt. (PDW), seedling vigor index (SVI I), seedling vigor index (SVI II), relative root elongation (RRE) and germination index (GI) (Figs. S2, S3, S4, and S5). All the seed germination parameters were measured on the sixth day after treatment (DAT) for both the varieties. Preliminary results obtained by seed germination assay suggested that the effective dose of B-AgNPs was 10 mg/L on the basis of RL, PL, SVI, RRE and GI parameters. The optimized concentration of 10 mg/L AgNPs as an early seedling growth promoter was further used in order to compare the efficacy of B-AgNPs with C-AgNPs, C-AgNPs + 10% FE and $AgNO_3$.

2.6.3. Reactive oxygen species (ROS) detection

Intracellular ROS in the plumule and radicle of 6 days old wheat seedlings were visualized using fluorescent molecular probe 2,7-dichlorofluorescein diacetate (H_2DCF-DA; Invitrogen; excitation 488 nm, emission 525 nm). 10 mg/L of AgNPs and $AgNO_3$ treated plumule and radicle of both wheat varieties were segmented and incubated in 20 μM H_2DCFDA [prepared in 10 mM Tris-HCl buffer (pH 7.4) from 20 mM stock solution, dissolved in dimethyl sulphoxide] for 30 min in dark at room temperature. Excess dye was removed by washing with MQ water and fluorescence intensity was recorded using Cell image analyzer (Thermo Scientific) equipped with 20X lens.

2.7. Cytotoxicity assay

Cytotoxicity assay was determined as per protocol reported by Tamás et al. (2004), using Evans blue staining. AgNPs, $AgNO_3$ treated and untreated control radicles were stained overnight in aqueous solution of 0.25% w/v Evans blue (Sigma, USA). Stained radicles were washed with MQ for 30 min and observed under a phase-contrast microscope (Leica DM- 2500, Wetzlar, Germany) at 40× magnifications (scale 50 μm) to assess root cell viability.

2.8. Silver content determination

The AgNPs treated seedling with MQ was washed with water thrice before the silver content detection in order to remove any traces of AgNPs from the surface of the seedlings. These seedlings were oven dried at 70 °C for 72 h. Nitric acid (60%):hydrofluoric acid (40%) in the ratio of 5:1 was added to the 0.1 g of wheat samples. It was digested in hot block digester (Kjeldhal-Digestion unit) for 6–8 h. The digests were finally diluted with MQ water and silver analysis was carried out. The total silver content in seedling was estimated on inductively coupled plasma mass spectrometry (ICP-MS) (Agilent technologies 7500cx) with three replicates.

2.9. Microscopy

Radicles were collected after application of 50 mg/L concentration of B-AgNPs suspension on day 6 for internalization of B-AgNPs at higher dose and processed for microscopy as described by Gonzalez-Melendi et al. (2008). Thin sections of radicles were observed under a phase-contrast microscope (Leica DM- 2500, Wetzlar, Germany) equipped with Leica Application Suite Version 4.2.0 (Leica Microsystems, Switzerland) at 10x and 40× magnifications (scale 50 μm), respectively.

2.10. Statistical analysis

The data obtained from experiments was expressed as the mean ± standard deviation (SD) of three replicates. Statistically significant differences between control and different treatments were analyzed using one-way analysis of variance (ANOVA) with Duncan's multiple range post hoc tests in all the cases ($p < 0.05$ was considered as significant using the SPSS 20.0 package software). The effects of different AgNPs and $AgNO_3$ treatments, varieties and their interaction with all the measured parameters were analyzed by linear mixed model multivariate ANOVA (M-ANOVA). Principal component analysis (PCA) was performed using “PAST” (PAleontological Statistics, Version 3.11) software.

3. Results and discussion

3.1. Mechanism of silver nanoparticles formation and stabilization

The stability of colloidal solution of silver nanoparticles is an important factor for their application. In order to prevent agglomeration, different types of stabilizing agents were used. The B-AgNPs suspension

used in present study was stable for more than 1 month without any sedimentation (Fig. S6). The well-dispersed B-AgNPs prepared by the reduction of Ag^+ using *P. emblica* extract which contain several biomolecules especially ascorbic acid which acts as reducing as well capping agent. The plausible mechanism of reduction and capping of silver nanoparticles by ascorbic acid is given in Supplementary data (Scheme S1). Xiong et al. (2011) reported that the lone pair of the hydroxyl group, π-electrons of the double bond and carbonyl group of lactone system in ascorbic acid molecule, provides enough reducing power to convert Ag^+ to AgNPs. Ascorbic acid acts as an electron as well as proton donor during reduction resulting in a radical species known as semidehydroascorbic acid which finally convert to dehydroascorbic acid. This ascorbic acid and dehydroascorbic acid form a redox system that had enough potential (~0.06 V) to reduce Ag^+ to Ag^0. Thsese silver nanoparticles were highly stabilized due to effective capping provided by biomolecules especially ascorbic acid as shown in Scheme S2 (Supplementary data).

3.2. UV-VIS spectral analysis

Bioreduction of Ag^+ to Ag^0 was studied as a function of time using UV-VIS spectrophotometer. Fig. 1a shows the UV-VIS spectra of diluted (X10) aqueous B-AgNPs solution at different time intervals (0–290 min). The surface plasmon resonance (SPR) band was centered at 420–440 nm. The increase in the intensity of SPR with time suggests the increase in concentration of B-AgNPs in solution which reached saturation after 290 min indicating the completion of the reaction.

The color of $AgNO_3$ aqueous solution changed from colorless to yellow and finally to dark brown upon addition of *P. emblica* fruit extracts (Fig. 1b). This characteristic color variation and λ_{max} at 420–440 nm are due to the excitation of the SPR confirm the formation of AgNPs. These results are in concurrence with earlier findings by Mohanta et al. (2016a); Nayak et al. (2016).

3.3. Scanning electron microscopy and EDX analysis

Fig. S7 (**a**) and **S7** (**b**) show the SEM images of synthesized silver nanoparticles at different magnifications. The image displays the spherical morphology of aggregated nanoparticle. The particles are separated by each other which is due to effective capping. EDX analysis is carried out to study the elemental composition B-AgNPs and result is shown in Fig. S7 (**c**). A peak at 3 keV confirms the formation of nanoparticles. The high intensity of the peak in EDX graph shows the purity of synthesized B-AgNPs (Vijayakumar et al., 2013). The other peak is due to the carbon of carbon tape used for sample preparation.

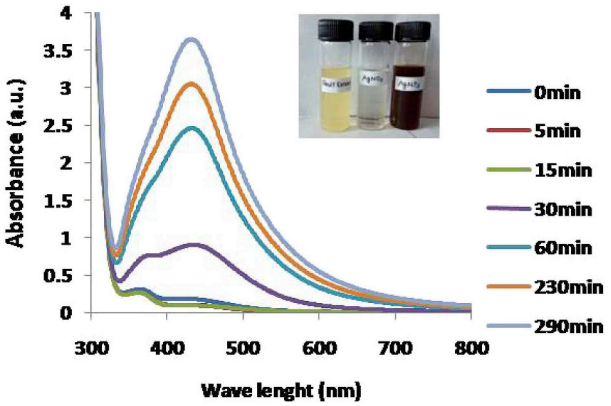

Fig. 1a. UV-VIS absorption spectra of synthesized B-AgNPs using *Phyllanthus emblica* L. (Amla) fruit extract at different time intervals.

3.4. High-resolution transmission electron microscopy (HR-TEM)

The morphology and particle size of B-AgNPs was analyzed by HR-TEM. HR-TEM study suggest the irregular shape with smooth edge morphology of B-AgNPs (Fig. 2). The particle size was in the range 10–35 nm, with an average size ~20 nm, which is in good agreement with the average crystallite size calculated from X-ray diffraction analysis. Leaf extract of *Memecylon umbellatum* used for the synthesis of silver nanoparticles and their size were found in the range of 15–20 nm (Arunachalam et al., 2013). Silver nanoparticles in the range of 1–30 nm are good candidate for bioactivity such as antimicrobial, antioxidant and anticancer as reported earlier (Mohanta et al., 2017b, 2018).

3.5. Zeta potential and dynamic light scattering (DLS)

Zeta potential and DLS measurements were carried out for B-AgNPs (Fig. S8 **a, b**). The zeta potential of B-AgNPs was found to be −23.8 mV (Fig. S8 a) indicating moderate stability and a good dispersion of AgNPs due to efficient capping. It has been reported that surface charge of pure AgNPs prepared by chemical route is about −27 mV (Mukherjee et al., 2014). The downward shifting of surface charge in B-AgNPs is due to the presence of capping molecules. The average size of B-AgNPs was between 25 and 40 nm (Fig. S8 b) as determined by DLS analysis. The size of B-AgNPs obtained by DLS measurement is in good agreement with the size obtained by HR-TEM analysis.

3.6. X-ray diffraction analysis

The XRD pattern of the biogenic AgNPs is given in Fig. 3. The well resolved peaks at 2θ: 38.18°, 44.42°, 64.18° and 70.38° corresponding to (111), (200), (220), and (311) planes respectively, suggest the cubic structure of B-AgNPs (space group Fm3m; a = 4.0740 Å, b = 4.0740 Å, c = 4.0740 Å, α = β = γ = 90°; JCPDS file no. 00-003-0921). The average crystallite size of B-AgNPs was calculated using the Debye-Scherrer formula (Eq. a) after subtracting the Cu K_α contribution and making allowance for instrumental broadening (Cullity, 1978).

$$D = K\lambda/\beta \cos\theta \quad \text{(a)}$$

Where D is the crystallite size of B-AgNPs, λ is the wave length of the X-ray source (0.1541 nm), β is the full width at half maximum of the diffraction peak, K is the Scherrer constant with a value from 0.9 to 1, and θ is the Bragg's angle. The average crystallite size was found to be 20 nm, which is in good agreement with the size obtained by SEM and HR-TEM technique.

3.7. Fourier transform infrared spectroscopy

FT-IR analysis of *P. emblica* extract was performed to identify the biomolecules responsible for reduction and stabilization of AgNPs. The FT-IR spectrum showed strong bands at 3348, 1637, 1138 and 1040 cm^{-1} (Fig. S9). The broad absorption band at 3348 cm^{-1} is due to O–H stretching of the phenol group while the band at 1638 cm^{-1} indicates the presence of conjugated carbonyl group (Isaac et al., 2013). The band at 1040-1086 cm^{-1} corresponds to C–N stretching vibration of aliphatic amines or C–O of alcohols/phenol (Mohanta et al., 2016b). B-AgNPs showed bands at 3450, 1637, 1383 and, 1086 cm^{-1}. The –OH stretching frequency appeared at 3450 cm^{-1} became less intense as compared to pure fruit extract probably due to the reduction in hydrophilicity, which confirms the capping of B-AgNPs.

3.8. DPPH (1,1-diphenyl-2-picryl hydroxyl) radical scavenging

The antioxidant activity of B-AgNPs and *P. emblica* fruit extract (FE) was evaluated by DPPH assay. DPPH free radical method is an

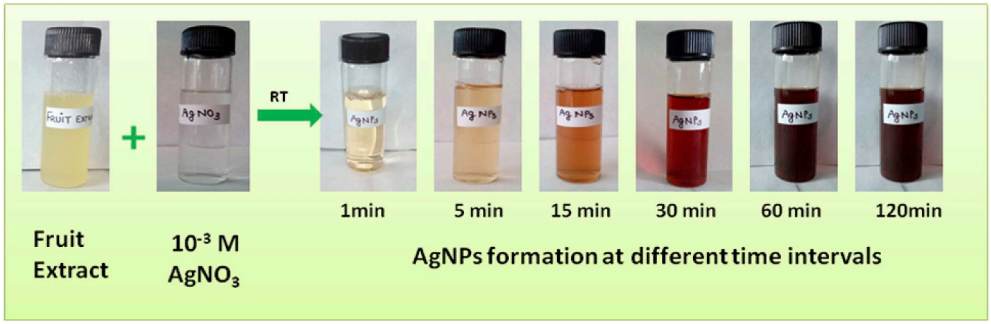

Fig. 1b. Visible observations of color change of reaction mixture during biosynthesis of AgNPs. (For interpretation of the references to color in this figure legend, the reader is referred to the Web version of this article.)

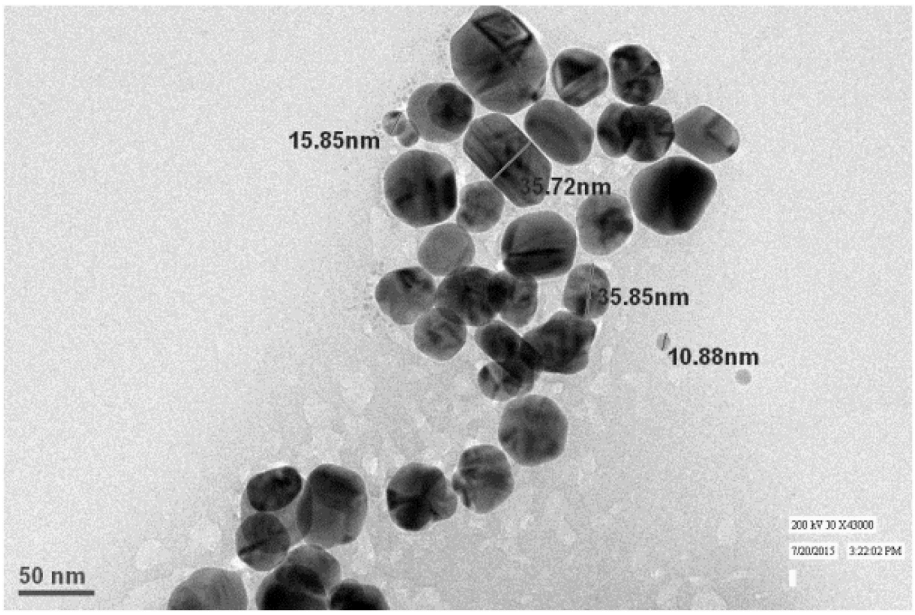

Fig. 2. HR-TEM images of biogenic silver nanoparticles (B-AgNPs).

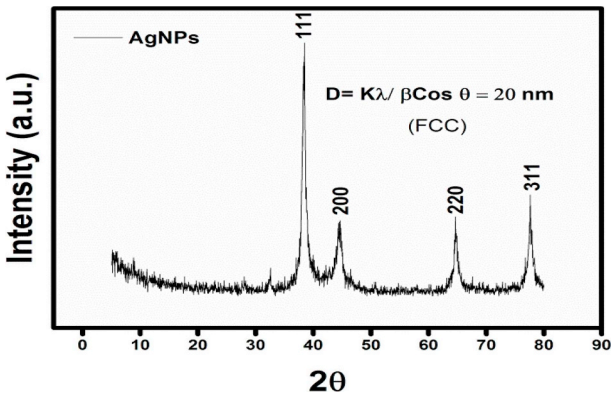

Fig. 3. X-ray diffraction spectrum (XRD) of stabilized biogenic silver nanoparticles.

antioxidant assay for rapid detection of antioxidants. Ascorbic acid was used as a positive control. The addition of FE and B-AgNPs in the DPPH solution led the color to change from purple to yellow, which might be attributed to the reduction of nitrogen-free radical to hydrazine. This is due to the presence of several phyto-reductant (natural antioxidants) present in the *P. emblica* fruit extract. The variation in % inhibition of DPPH radical with different concentrations of FE, B-AgNPs, and ASA are shown in Table S1. The increase in concentration from 1 to 50 μg/mL resulted in an increase in the % inhibition. This value was found to be 35.35–91.49% for ascorbic acid, 26.4–90% for FE, & 35.48–91.93% for B-AgNPs (Table S1).

The IC_{50} (μg/ml) values of control, *P. emblica* fruit extract, and B-AgNPs were found to be 9.88 ± 0.71, 14.51 ± 0.31 and 10.02 ± 0.79, respectively (Table S1). The IC_{50} value for B-AgNPs was lower which represent the higher potential antioxidant activity. The radical scavenging ability of B-AgNPs further confirmed the presence of natural antioxidant on the surface of AgNPs which plays an important role in mitigating the ROS stress of the wheat seedlings.

3.9. Effect of different AgNPs and $AgNO_3$ treatments on reactive oxygen species (ROS)

ROS are generated as a byproduct of several metabolic activities during seed germination, growth of seedling and whole life cycle of the plant. The high production of ROS can lead to toxicity in plants (Sharma et al., 2012; Gomes and Garcia, 2013). Keeping this in view, we studied the effect of optimized dose of B-AgNPs (10 mg/L) on ROS generation in the germinating seeds of two wheat varieties using DCF-DA stain (Figs. 4 and 5). The B-AgNPs treated plumule and radicles showed minimum production of ROS as compared to other AgNPs (Fig. 4 **B, G;** Fig. 5B, G). $AgNO_3$ treated seeds showed the strongest green fluorescence compared to other AgNPs treated seeds for both the varieties [Fig. 4 (**E, J**) and Fig. 5 (**E, J**)]. The increase in ROS accumulation in radicles and plumules was found in the order $AgNO_3$ > C-AgNPs > C-AgNPs + 10% FE > control > B-AgNPs for both varieties. However,

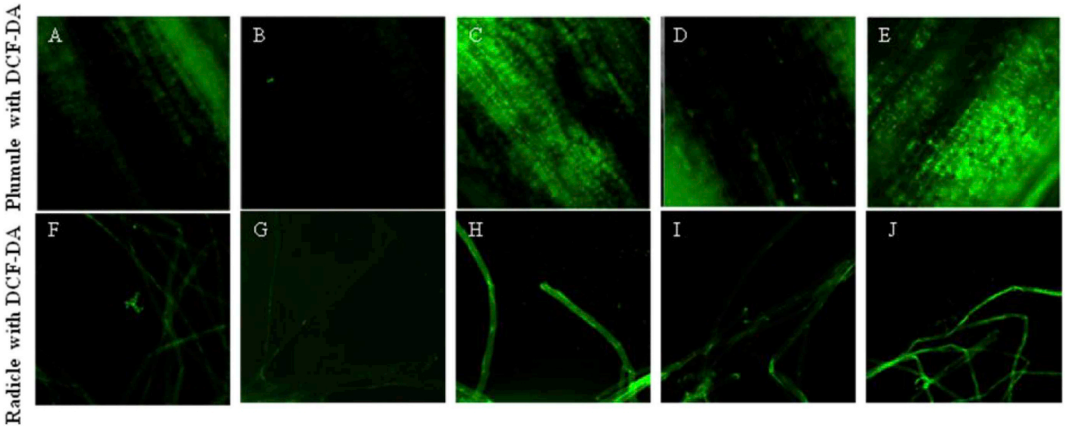

Fig. 4. Effect of AgNPs and $AgNO_3$ treatment (10 mg/L concentration) on reactive oxygen species (ROS) production in plumule and radicles of wheat seedlings (HD-2967) at 6 DAT (A, F represent control, B, G represent B-AgNPs, C, H represent C-AgNPs, D, I represent C-AgNPs +10FE and E, J represent $AgNO_3$ treatments for plumules and radicles, respectively).

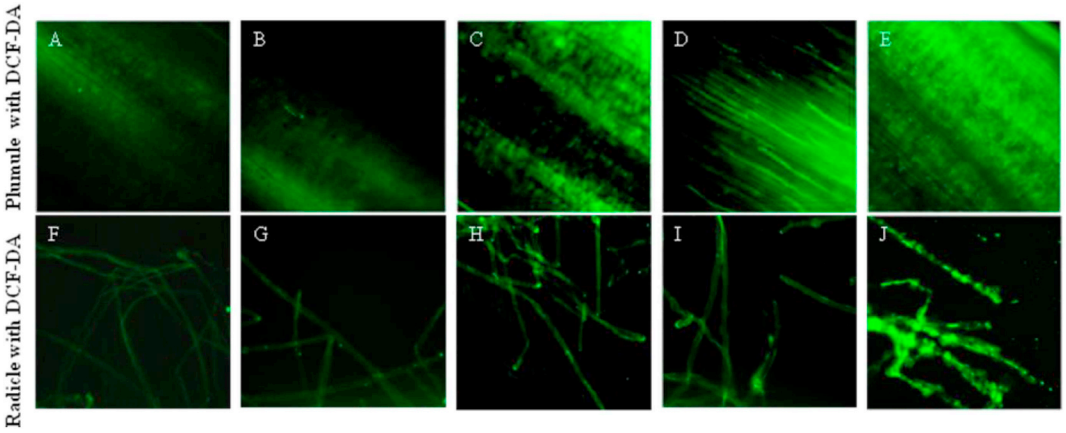

Fig. 5. Effect of AgNPs and $AgNO_3$ treatment (10 mg/L concentration) on reactive oxygen species (ROS) production in plumule and radicles of wheat seedlings (DBW-17) at 6 DAT (diagram A, F, represent control, B, G, represent B-AgNPs, C, H, represent C-AgNPs, D, I, represent C-AgNPs +10FE and E, J, represent $AgNO_3$ treatments for plumules and radicles, respectively).

ROS production in DBW-17 was higher as compared to HD-2967 when they treated with B-AgNPs. Untreated, C-AgNPs as well as $AgNO_3$ treated DBW-17 variety produced higher ROS which resulted in reduced seedling growth. In the case of C-AgNPs and $AgNO_3$ treatments, over production of ROS could be due to the intracellular agglomeration of Ag^+ in seedlings which resulted in increased oxidative stress (Yasur and Rani, 2013). A similar observation was reported by Cvjetko et al. (2018) where ROS accumulation was higher in Tobacco root tips treated with $AgNO_3$ as compared to AgNPs. However, in control (untreated seeds), excessive ROS accumulation and reduction in seedling growth was found, possibly due to disturbance or inadequate antioxidative defense mechanism. Such observations were also reported by Sharma et al. (2012). Maximum seedling growth and minimum ROS generation were observed in B-AgNPs treatment which is due to effective antioxidative defense induced by phytochemicals capped AgNPs (Gupta et al., 2018). These results concur with the findings of Ma et al. (2015), who also observed that AgNPs induced nanotoxicity in *Crambe abyssinica* can be reduced by the enhanced expression of glutathione (GSH) and related peptides.

3.10. 10. Impact of AgNPs and $AgNO_3$ on seed germination and early seedling growth in wheat

3.10.1. Effect of different AgNPs and $AgNO_3$ treatments on seed germination percentage of two wheat varieties

Seed germination percentage was not affected by B-AgNPs treatment as compared to untreated in wheat varieties (Fig. S10). Both varieties showed 100% germination for both control as well as B-AgNPs treated seeds. The only difference was found in $AgNO_3$ treated seeds where 80% and 50% germination was found for HD-2967 and DBW-17, respectively. In case of other AgNPs treated seeds, there was significant reduction ($P < 0.05$) in germination percentage which was found to be 23.25%, 10.0% for HD-2967 treated with C-AgNPs and C-AgNPs + 10% FE respectively. A significant reduction ($P < 0.05$) was recorded in variety DBW-17 as compared to control (Fig. S10). AgNPs having a the size less than 100 nm are known to adversely affect the growth of *Cucurbita pepo* plant resulting in the reduction of biomass (Stampoulis et al., 2009). Furthermore, Amooaghaie et al. (2015) found that 0.2–1.6 mg/L AgNPs were sufficient to suppress the seed germination of *Brassica nigra* seeds and seedlings. The observed phytotoxic effects of the silver nanoparticles were due to the re-oxidation of Ag^0 to Ag^+ ions. It is reported that Ag^+ has inhibitory effects on seed germination and seedling growth since it can inactivate proteins and enzymes (Vannini et al., 2014).

3.10.2. Impact of biogenic AgNPs (B-AgNPs) treatment on seedling growth of two wheat varieties

Effects of different concentrations (0, 5, 10, 25 and 50 mg/L) of B-AgNPs on seed germination percentage and early seedling growth on both varieties are shown in Figs. S11–S12. Maximum increments in all seed germination parameters were recorded at the concentration of 10 mg/L. It was also found that the increments were higher in HD- 2967

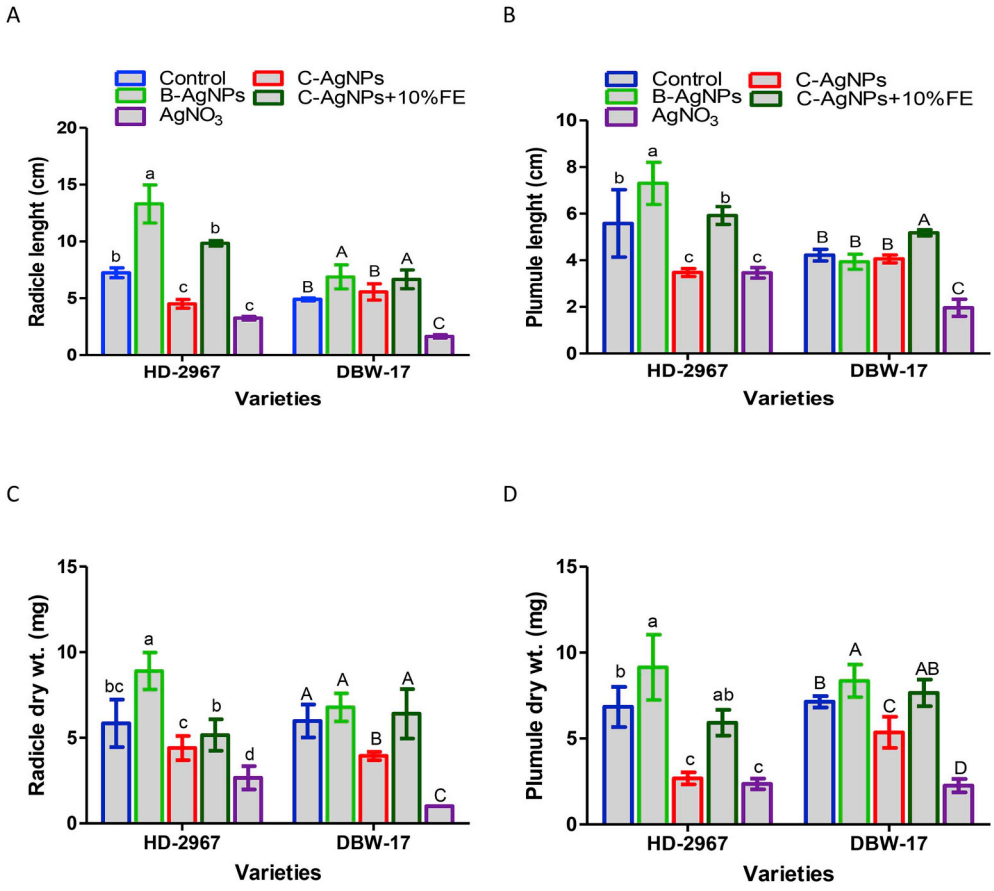

Fig. 6. Variations in seed germination parameters, radicle length (RL), plumule length (PL), radicle dry weight (RDW) and plumule dry weight (PDW) at 10 mg/L AgNPs and $AgNO_3$ treated wheat varieties (HD-2967 and DBW-17) at 6 days after treatment. Significant results of one-way ANOVA are shown ($P < 0.05$) with in varieties (var), for AgNPs and $AgNO_3$ treatments. Letters indicate differences between treatments within each variety ($P < 0.05$).

than DBW-17. At 6 DAT, the radicle length (RL) of HD-2967 treated with 5, 10 and 25 mg/L B-AgNPs solutions, was increased ($P < 0.001$) by 66.02%, 83.7% and 73.75%, respectively. While in case of DBW-17, it was increased by 48.97%, 40.40%, and 9.79%, respectively as compare to control (Fig. S11B). Relative root elongation (RRE) was increased significantly in both the varieties. It was found to be 68.12%, 82.13%%, 65.77% for HD-2967, and 39.92%, 53.63%, and 12.84% for DBW-17 variety respectively after treatment with 5, 10 and 25 mg/L B-AgNPs (Fig. S12G). B-AgNPs treated seeds showed a significant enhancement in germination index (GI). It was found to be 68.13%, 82.13% and 65.77% for HD-2967 and 53.62%, 55.46% and 25.38% for DBW-17 as compared to control (Fig. S12H). It was also observed that the RL, PL SB, SVI, RRE, and GI were insignificantly reduced in HD-2967 seeds treated with 50 mg/L B-AgNPs. However, in variety DBW-17, these parameters significantly decreased ($P < 0.01$) and found to be 44.48%, 43.12%, 25.91%, 36.84%, 43.28%, and 36.97% respectively as compared to the control at 6 DAT (Figs. S3, S4, S5). These results suggest that the phytochemicals capped AgNPs are non-toxic due to the surface coating of B-AgNPs with natural antioxidant which may promote root elongation and seedling growth. Similar results were reported for seeds treated with biosynthesized AgNPs by Yasur and Rani (2013); Ushahra et al. (2014); Gupta et al. (2018). Natural antioxidants of *P. emblica* such as ascorbic acid and hydrolyzable tannins are known to be effective for scavenging ROS (Scartezzini et al., 2006). The bioactive constituents present in the plant extract not only acts as a stabilizing agent but also enhances the biocompatibility of AgNPs (Moulton et al., 2010). At a crucial phase of seed germination, antioxidants play an important role as they balance redox status and mitigate oxidative stress (De Tullio and Arrigoni, 2003). It is quite possible that natural antioxidant capped AgNPs might penetrate the seed coat due to the small size and deliver the desired amount of natural antioxidants that results in a significant increase in seed germination. Khodakovskaya et al. (2009) also reported that carbon nanotubes (CNT) were able to penetrate the thick seed coat of tomato seeds and enhanced the water uptake inside seed which effect seed germination and seedling growth. Recently, Mahakham et al. (2016) reported that phytochemically capped GNPs act as nano priming agent and promoted seed germination and seedling growth of maize plants. It is interesting to note that B-AgNPs exhibited dose-dependent seed germination and seedling growth for both wheat varieties. Maximum growth of the seedlings in both the varieties was found at 10 mg/L concentration of B-AgNPs. Beyond this concentration, reduction in seed germination parameters wasinsignificant (50 mg/L). The reduction in seed germination parameters at high AgNPs concentration could be due to the aggregation of NPs (Ma et al., 2010). Agglomeration of B-AgNPs at 50 mg/L in the cortex region of roots is shown in Fig. S13 **D and 13E**. These B-AgNPs agglomeration may hinder the movement of nutrients and biomolecules which are essential for normal growth of seedlings. Razack et al. (2016) reported that at higher concentrations, the agglomeration of AgNPs hindered the galactose metabolism pathway ultimately resulting in cell wall damage. Furthermore, EDX analysis showed a characteristic peak at 3 KeV, confirming the presence of AgNPs aggregates in radicals of wheat seedling treated with B-AgNPs solution (concentration; 50 mg/L) (Fig. S13 **C, F**). Several other studies have shown the internalization, accumulation, and translocation of nanoparticles in plants (Gonzalez-Melendi et al., 2008; Mahakham et al., 2016; Palocci et al., 2017). Gonzalez-Melendi et al. (2008) reported the presence of carbon-coated Fe nanoparticles inside *Cucurbita pepo* by using several microscopic techniques, including phase contrast microscopy. Furthermore, Cifuentes et al. (2010) reported accumulation of magnetic carbon coated nanoparticles in four crops i.e. sunflower, tomato, pea, and wheat.

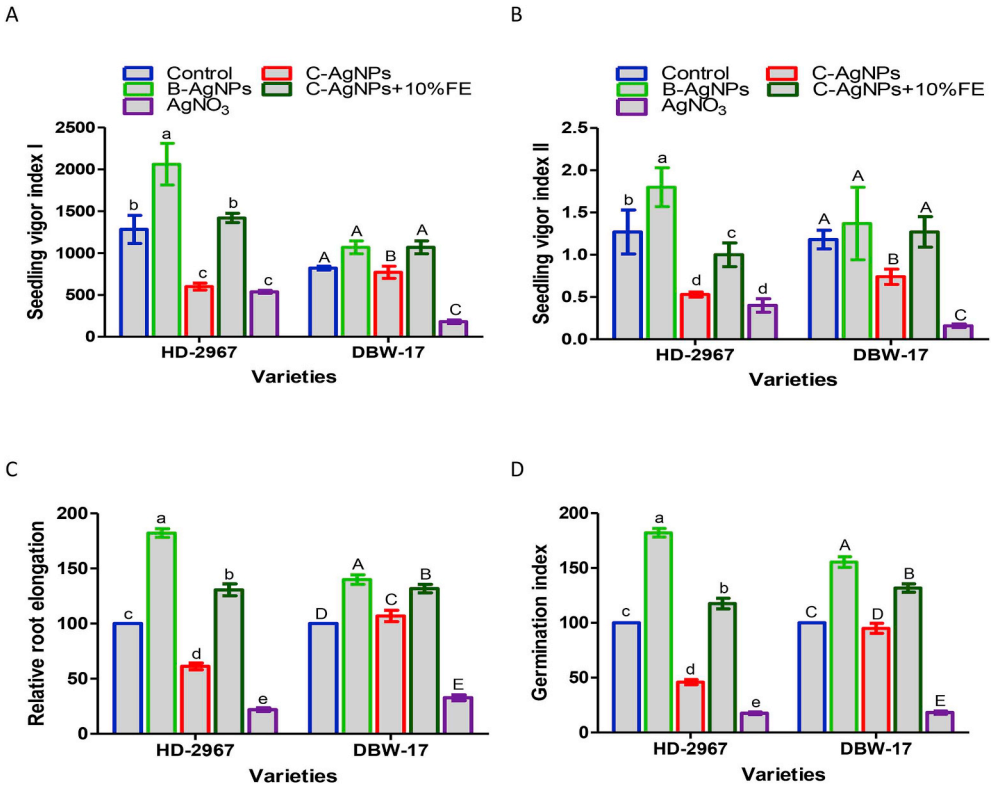

Fig. 7. Variations in seed germination parameters, seedling vigor index I (SVI I), seedling vigor index II (SVI II), relative root elongation (RRE) and germination index (GI) at 10 mg/L AgNPs and $AgNO_3$ treated wheat varieties (HD-2967 and DBW-17) at 6 days after treatment. Significant results of one-way ANOVA are shown ($P < 0.05$) with in varieties (var), for AgNPs and $AgNO_3$ treatments. Letters indicate differences between treatments within each variety ($P < 0.05$).

Table 1
F values and significance levels for different AgNPs treatments and $AgNO_3$ treatment at 10 mg/L concentration for various seed germination parameters in two wheat (*Triticum aestivum* L.).

Parameters	Trt (TRT)	Varieties (VR)	TRT x VR
RL (cm)	89.319***	72.166***	46.853***
PL (cm)	80.533***	141.127***	52.719***
RDW (mg)	5.772*	8.172*	3.099*
PDW (mg)	7.595**	1.679^{ns}	2.421 ^{ns}
SB (mg)	10.716**	0.700 ^{ns}	3.106*
SVI (%)	234.353***	422.736***	110.651***
RRE (%)	341.957***	6.454*	107.593***
GI	357.783***	38.821***	96.873***

VR variety; *TRT* treatment; *RL* radicle length; *PL* plumule length; *RWD* radicle dry, *PDW* plumule dry weight, *SB* Seedling biomass, *SVI* seedling vigor index; *RRE* relative root elongation; *GI* germination index; ***p < 0.001; **p < 0.01; *p < 0.05 (level of significance); ns non-significant.

3.10.3. Phytotoxicity evaluation of biologically synthesized AgNPs vs chemically synthesized AgNPs, and $AgNO_3$ in terms of growth parameters

Phytotoxicity of silver nanoparticles (B-AgNPs, C-AgNPs, C-AgNPs +10% FE and $AgNO_3$ salt) on seed germination and early seedling growth was studied on two wheat varieties after 6 days of treatment (Figs. 6 and 7). B-AgNPs (concentration; 10 mg/L) treated seeds showed significant enhancement ($P < 0.001$) in RL, PL, RDW, PDW, SVI- I, SVI- II, RRE and GI by 194.90%, 110%, 102.27%, 241%, 243.93%, 239.73%, 197.67% and 296.87% respectively for HD-2967 (Figs. 6 and 7), whereas C-AgNPs treated DBW-17 seeds showed an increment ($P < 0.01$) in RL, PL,RDW, PDW,SVI- I, RRE and GI by 31.37%, 26.10%, 72.08%, 62.31%, 41.73%, 43.76% and 63.67% (Figs. 6 and 7) respectively. C-AgNPs treated HD-2967 seeds showed significant ($P < 0.001$) decrease in RL, PL, RDW, PDW, SVI-I, SVI-II, RRE and GI (Figs. 6 **and 7**) by 37.70%, 37%, 60.81%, 44.16%, 58.12%, 38.81%, 54.10% and 23.25% respectively as compared to the control. In DBW-17 significant reduction was recorded only in RDW, PDW, SVI-II parameters (Table S2).

C-AgNPs + 10% FE treated HD-2967 seeds showed significant enhancement ($P < 0.05$) in RL, SVI-I, RRE, and GI by 35.91%, 10.63%, 30.64% and 17.58% respectively. However decrease was recorded in case of RDW, PDW, SB, and SVI-II. An increase in RL, SL, SDL, SVI-I, RRE, and GI by 35.91%, 22.74%, 29.82%, 29.82%, 31.7% and 31.71% respectively observed in DBW-17 treated seeds (Figs. 6 and 7). All seed germination parameters were significantly ($P < 0.05$) decreased in case of $AgNO_3$ treated seeds (Figs. 6 and 7). It is reported that chemically synthesized AgNPs induces toxicity in terms of decrease in the size of roots and shoot growth, excessive generation of ROS, increased oxidative stress and cell damage in rice seedlings (*Oryza sativa* L.), (Mirzajani et al., 2014; Thuesombat et al., 2014). The toxicity in plants can be caused by the adsorption of harmful chemicals on the surface of nanoparticles during their chemical synthesis (Krishnaraj et al., 2012). In contrast to these negative impacts, B-AgNPs showed a positive growth effect on wheat seedlings. Similar phytostimulatory effect of biosynthesized AgNPs on rice seedling growth has also reported by Gupta et al. (2018).

Results of multivariate ANOVA clearly depict that both varieties showsignificant variations in response to different AgNPs and $AgNO_3$ treated seeds as compared to control (Table 1). Under different AgNPs and $AgNO_3$ exposure, the result of multivariate ANOVA showed that RL, PL, SVI, RRE and GI varied significantly ($p < 0.001$) due to TRT, VR, and their interactions. RDW varied significantly ($p < 0.05$) due to TR, VR, and TRT x VR. PDW and SB varied significantly due to TRT ($p < 0.01$) (Table 1).

PCA analysis was carried out to compare and validate the findings of seed germination percentage and seedling growth after treatment of AgNPs and $AgNO_3$ solution (concentration; 10 mg/L) in both wheat varieties. Fig. S14 shows the biplot for wheat varieties and their interaction with different treatments. PCA analysis revealed the two principal components which were responsible for the 96.96% variance in both the wheat varieties. The first principal component (PC1) shares 90.13% while the second (PC2) shares 6.83% of the data matrix (Fig. S14). The maximum positive loadings on PC1 were of germination index (GI), seedling vigor index (SVI), relative root elongation (RRE),

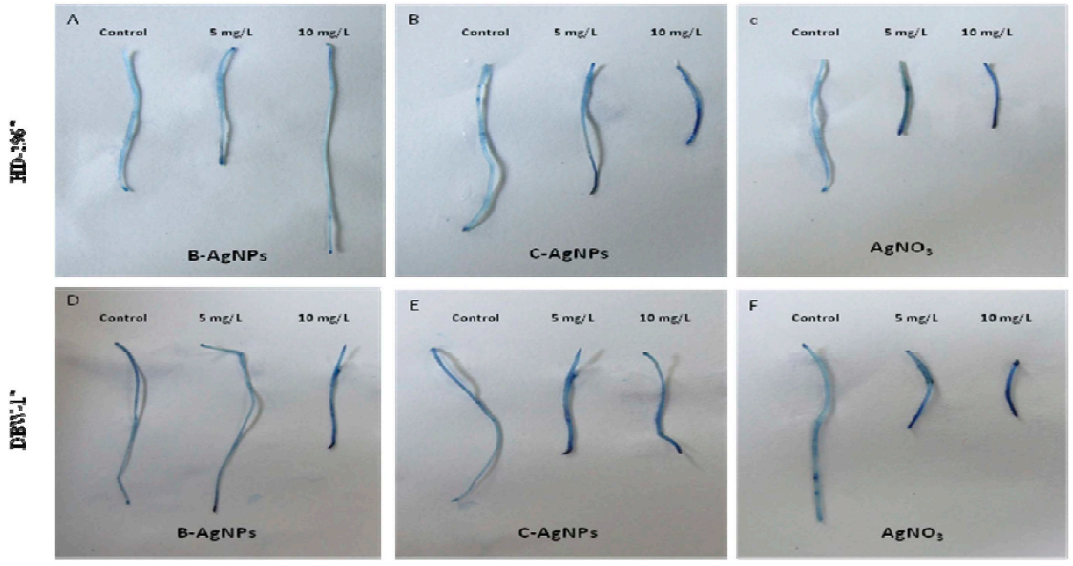

Fig. 8a. Cytotoxicity assay in radicles stained with Evans blue dye indicates root cell viability in wheat varieties (HD-2967 and DBW-17) at 6 DAT under different treatments. Diagram A, D, represent B-AgNPs, B, E, represent C-AgNPs, and C, F, represent $AgNO_3$ treatments, respectively). (For interpretation of the references to color in this figure legend, the reader is referred to the Web version of this article.)

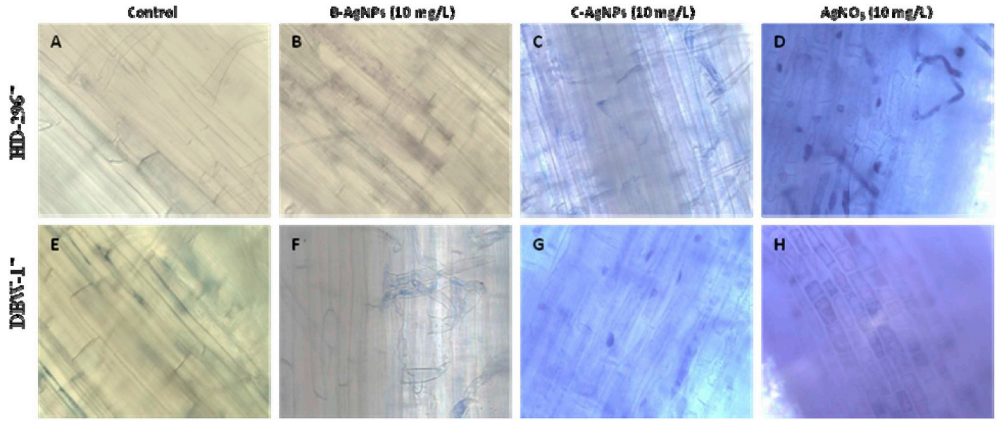

Fig. 8b. Enlarge microscopic view (40x) of Evans blue stained radicles (dark blue spots) in wheat varieties (HD-2967 and DBW-17) at 6 DAT. (For interpretation of the references to color in this figure legend, the reader is referred to the Web version of this article.)

Table 2
Bioaccumulation of Ag content (mg Kg^{-1} dry weight) in seedlings of two wheat varieties (*Triticum aestivum* L.) different AgNPs and $AgNO_3$ (10 ppm conc.) for 6 DAT compared to control.

Ag Content (mg Kg^{-1})		
	HD-2967	DBW-17
Control	0.0051 ± .002	0.0037 ± .002
B-AgNPs	1.86 ± 0.133***	1.76 ± 0.119***
C-AgNPs	7.14 ± 0.085***	14.13 ± 1.94**
C-AgNPs + 10%FE	5.19 ± 0.104***	5.02 ± 0.092***
$AgNO_3$	20.33 ± 1.93**	12.52 ± 2.08**

Data are means ± standard deviation, n = 3.. $*P < 0.05$; $**P < 0.01$, $***P < 0.001$.

and radicle length (RL) (Fig. S14 **b&c**). It is evident that control, B-AgNPs and C-AgNPs +10%FE were falling in one group for HD-2967 variety, whereas it have similar responses for DBW-17 variety (Fig. S14 a). $AgNO_3$ and C-AgNPs treated seeds were differ from each other. However, C-AgNPs and $AgNO_3$ treated seeds showed variations in both the varieties. PCA analysis suggested that the variables such as radicle length (RL), seedling vigor index (SVI), relative root elongation (RRE), and germination index (GI) are responsible for cluster separation.

It was interesting to note that C-AgNPs treated seeds showed inhibitory effect on root elongation and seedling growth in both the varieties as compared to control. However, the addition of 10% *P. emblica* fruit extract to C-AgNPs significant improvement was observed in seed germination percentage, radicle length, and plumule length ($P < 0.05$). This clearly shows that *P. emblica* extract act as an efficient ROS scavenger. The major causes for the reduction in seedling growth and seedling biomass in both the varieties in the case of C-AgNPs are back oxidation of Ag to Ag^+ ions which arises due to lack of capping and higher ROS generation. Thwala et al. (2013) reported the toxicity of AgNPs and ZnO due to the dissolution of particular ions in *Spirodela punctuta*. It is reported that Ag^+ ions cause very toxic effects on the growth of the seedlings as they form complex with several essential biomolecules that disrupt normal physiology and growth of the seedlings (Stampoulis et al., 2009; Vannini et al., 2013). The process of dissolution of AgNPs to Ag^+ depends on some important physiochemical parameters such as size and concentration of nanoparticles, pH, temperature, ionic strength and presence of ligands (McGillicuddy et al., 2017). Present results indicated that two wheat varieties showed different response towards AgNPs treatments as HD-2967 variety was highly responsive to B-AgNPs treatments as compared to DBW-17

variety. B-AgNPs can act as a growth promoter at 10 mg/L concentration by alleviating harmful ROS generation as compared to control in both wheat varieties. Further studies will be required to understand the complex interaction of AgNPs at molecular and physiological levels during seed germination and seedling growth.

3.10.4. Cytotoxicity assay by Evans blue dye

Cytotoxicity of treated and untreated root cells of wheat was studied by root cell viability assay using Evans blue dye. This dye is a marker of membrane cells integrity (Gaff and Okongo'ogola, 1971). Fig. 8 (a) and 8 (b) depicts Evans blue dye stained images of control radicle as well as radicle treated with 5 mg/L & 10 mg/L concentrations of B-AgNPs, C-AgNPs and $AgNO_3$. Root cell viability was found maximum in case of B-AgNPs treated HD-2967 radicles followed by control, C-AgNPs and $AgNO_3$, respectively. However in DBW-17, maximum root cell viability was found in control close to B-AgNPs treated radicle. It might be due to the surface coating of B-AgNPs by phytochemicals present in *P. emblica* fruit extract. Higher uptake of dye by radicles of both the wheat varieties treated with 10 mg/L $AgNO_3$ solution as compared to control indicates significant root cell death (Fig. 8 b). Wang et al. (2011) found that chemically synthesized CuO nanoparicles causes loss of cell integrity in maize roots. Suspension of CuO nanoparticles (1.5 mM) also showed a detrimental effect on rice root cells stained with Evans blue (Shaw and Hossain, 2013).

3.10.5. Silver content (Ag) accumulation studies in wheat seedlings

Wheat seedlings of untreated seeds, as well as seeds treated with different solutions (10 mg/L) of B-AgNPs, C-AgNPs, C-AgNPs + 10%FE and $AgNO_3$, were digested (HNO_3:HF) for silver content detection by ICP-MS analysis at 6 DAT. Accumulation of silver content in B-AgNPs was lower than those of C-AgNPs and C-AgNPs + 10%FE treated seedlings (Table 2). In HD-2967 variety, silver content was found to be 1.86 mg kg^{-1}, 7.14 mg kg^{-1}, 5.19 mg kg^{-1}, 20.33 mg kg^{-1} for B-AgNPs, C-AgNPs, C-AgNPs + 10%FE and $AgNO_3$ treated seedlings respectively. However, in case of DBW-17, it was 1.76 mg kg^{-1}, 14.13 mg kg^{-1}, 5.02 mg kg^{-1}, 12.52 mg kg^{-1} for B-AgNPs, C-AgNPs, C-AgNPs + 10%FE and $AgNO_3$ treatments respectively. The highest silver content was detected in $AgNO_3$ treatment, while in untreated (control) amount of accumulated Ag was below the detection limit of ICP-MS. These results are similar to the findings reported by other researchers. Pokhrel and coworker reported that the higher phytotoxicity of $AgNO_3$ than AgNPs and ZnO nanoparticles in maize (Pokhrel and Dubey, 2013), Allium (Cvjetko et al., 2017) plants. In present study, higher Ag content was found in seed treated with $AgNO_3$ is due to fact that Ag^+ ions form stable complex with biomolecules that induce oxidative stress in seeds (Fig. 4 **(E, J)** & Fig. 5 **(E, J)**). It is also reported by Xu et al. (2010) that higher ROS content results in reduced seedling growth.

4. Conclusion

Biogenic silver nanoparticles have been successfully synthesized and characterized. The results of present study demonstrates the potential role of biogenic AgNPs in wheat as a growth promoter without any toxic effect which is generally associated with chemically synthesized AgNPs. Exogenous application of phytochemicals capped AgNPs (concentration; 10 mg/L) promotes the growth of the wheat seedlings by providing protection against oxidative stress as concluded from increased biomass, relative root elongation, and higher root cell viability. Enhancement in the seed germination by administrating natural antioxidant through the B-AgNPs will open a new way for the delivery of active molecules to mitigate ROS toxicity for sustainable agriculture production.

Author's contribution

VPA (Vivek Pandey), VPR (Vivek Prasad) and RK designed the experiment. RK and CMS did the synthesis and characterization of AgNPs. BNS did ROS detection work. VPA and RK analyzed the data. RK, VPA, VPR wrote the paper.

Conflicts of interest

The authors declared that there is no conflict of interests regarding the publication of this manuscript.

Acknowledgments

The authors gratefully acknowledge Delhi Technological University (DTU), Delhi, for providing the characterization facilities. The authors are thankful to Director, CSIR-NBRI, Lucknow for providing necessary facilities. We acknowledge Council of Scientific and Industrial Reseach (CSIR), Govt of India for funding this work under NBRI in-house project no. OLP-103.

Appendix A. Supplementary data

Supplementary data to this article can be found online at https://doi.org/10.1016/j.plaphy.2019.08.008.

References

Abdul-Baki, A.A., Anderson, J.D., 1973. Vigor determination in Soybean seed by multiple criteria. Crop Sci. 13, 630–633. https://doi.org/10.2135/cropsci1973.0011183X001300060013x.

Ahmed, S., Ahmad, M., Swami, B.L., Ikram, S., 2016. A review on plants extract mediated synthesis of silver nanoparticles for antimicrobial applications: a green expertise. J. Adv. Res. 7 (1), 17–28.

Amooaghaie, R., Saeri, M.R., Azizi, M., 2015. Synthesis, characterization and biocompatibility of silver nanoparticles synthesized from *Nigella sativa* leaf extract in comparison with chemical silver nanoparticles. Ecotoxicol. Environ. Saf. 120, 400–408. https://doi.org/10.1016/j.ecoenv.2015.06.025.

Ankamwar, B., Damle, C., Ahmad, A., Sastry, M., 2005. Biosynthesis of gold and silver nanoparticles using *Emblica officinalis* fruit extract, their phase transfer and transmetallation in an organic solution. J. Nanosci. Nanotechnol. 5 (10), 1665–1671.

Arunachalam, K.D., Annamalai, S.K., Hari, S., 2013. One-step green synthesis and characterization of leaf extract-mediated biocompatible silver and gold nanoparticles from *Memecylon umbellatum*. Int. J. Nanomed. 8, 1307–1315. https://doi.org/10.2147/IJN.S36670.

Bailly, C., El-Maarouf-Bouteau, H., Corbineau, F., 2008. From intracellular signaling networks to cell death: the dual role of reactive oxygen species in seed physiology. C. R. Biol. 331, 806–814. https://doi.org/10.1016/j.crvi.2008.07.022.

Barrena, R., Casals, E., Colón, J., Font, X., Sánchez, A., Puntes, V., 2009. Evaluation of the ecotoxicity of model nanoparticles. Chemosphere 75, 850–857. https://doi.org/10.1016/j.chemosphere.2009.01.078.

Chhipa, H., Joshi, P., 2016. Nanofertilisers, nanopesticides and nanosensors in agriculture. In: Nanoscience in Food and Agriculture, vol. 1. Springer International Publishing, Cham, pp. 247–282. https://doi.org/10.1007/978-3-319-39303-2_9. 247–282.

Choi, C.W., Kim, S.C., Hwang, S.S., Choi, B.K., Ahn, H.J., Lee, M.Y., et al., 2002. Antioxidant activity and free radical scavenging capacity between Korean medicinal plants and flavonoids by assay-guided comparison. Plant Sci. 163, 1161–1168. https://doi.org/10.1016/S0168-9452(02)00332-1.

Cifuentes, Z., Custardoy, L., de la Fuente, J.M., Marquina, C., Ibarra, M.R., Rubiales, D., Pérez-de-Luque, A., 2010. Absorption and translocation to the aerial part of magnetic carbon-coated nanoparticles through the root of different crop plants. J. Nanobiotechnol. 8, 26. https://doi.org/10.1186/1477-3155-8-26.

Cullity, B.D., 1978. Elements of X-Ray Diffraction, second ed. Addison-Wesley, London, pp. 102.

Cvjetko, P., Milošić, A., Domijan, A.M., Vinković-Vrček, I., Tolić, S., Peharec-Štefanić, P., et al., 2017. Toxicity of silver ions and differently coated silver nanoparticles in *Allium cepa* roots. Ecotoxicol. Environ. Saf. 137, 18–28. https://doi.org/10.1016/j.ecoenv.2016.11.009.

Cvjetko, P., Zovko, M., Štefanić, P.P., Biba, R., Tkalec, M., Domijan, A.M., et al., 2018. Phytotoxic effects of silver nanoparticles in tobacco plants. Environ. Sci. Pollut. Res. 25, 5590–5602.

De Tullio, M.C., Arrigoni, O., 2003. Invited review and research opinion the ascorbic acid system in seeds: to protect and to serve. Seed Sci. Res. 13, 249–260. https://doi.org/10.1079/SSR2003143.

Esfanddarani, H.M., Kajani, A.A., Bordbar, A.K., 2017. Green synthesis of silver nanoparticles using flower extract of *Malva sylvestris* and investigation of their antibacterial activity. IET Nanobiotechnol. 12 (4), 412–416.

Farkas, J., Peter, H., Christian, P., Urrea, J.A.G., Hassellöv, M., Tuoriniemi, J., et al., 2011. Characterization of the effluent from a nanosilver producing washing machine. Environ. Int. *37* (6), 1057–1062.

Gaff, D.F., Okongo'ogola, O., 1971. The use of non-permeating pigments for testing the survival of cells. J. Exp. Bot. 22, 756–758.
Geethalakshmi, R., Sarada, D.V.L., 2010. Synthesis of plant-mediated silver nanoparticles using *Trianthema decandra* extract and evaluation of their anti microbial activities. Int. J. Eng. Sci. Technol. 2, 970–975. https://doi.org/10.1155/2011/573429.
Gogos, A., Knauer, K., Bucheli, T.D., 2012. Nanomaterials in plant protection and fertilization: current state, foreseen applications, and research priorities. J. Agric. Food Chem. 60 (39), 9781–9792.
Gomes, M., Garcia, Q., 2013. Reactive oxygen species and seed germination. Biologia (Bratisl) 68, 351–357. https://doi.org/10.2478/s11756-013-0161-y.
Gonzalez-Melendi, P., Fernandez-Pacheco, R., Coronado, M.J., Corredor, E., Testillano, P.S., Risueno, M.C., et al., 2008. Nanoparticles as smart treatment-delivery systems in plants: assessment of different techniques of microscopy for their visualization in plant tissues. Ann. Bot. 101, 187–195. https://doi.org/10.1093/aob/mcm283.
Gupta, S.D., Agarwal, A., Pradhan, S., 2018. Phytostimulatory effect of silver nanoparticles (AgNPs) on rice seedling growth: an insight from antioxidative enzyme activities and gene expression patterns. Ecotoxicol. Environ. Saf. 161, 624–633.
He, J., Dua, Y., Hua, D., Fan, G., Wang, L., Liu, Y., et al., 2012. DEXH box RNA helicase-mediated mitochondrial reactive oxygen species production in Arabidopsis mediates crosstalk between abscisic acid and auxin signaling. Plant Cell 24, 1815–1833. https://doi.org/10.1105/tpc.112.098707.
He, Y., Wei, F., Ma, Z., Zhang, H., Yang, Q., Yao, B., et al., 2017. Green synthesis of silver nanoparticles using seed extract of *Alpinia katsumadai*, and their antioxidant, cytotoxicity, and antibacterial activities. RSC Adv. 7 (63), 39842–39851.
Isaac, R.S.R., Sakthivel, G., Murthy, C., 2013. Green synthesis of gold and silver nanoparticles using *Averrhoa bilimbi* fruit extract. J. Nanotechnol. 906592–906597.
Khodakovskaya, M., Dervishi, E., Mahmood, M., Xu, Y., Li, Z., Watanabe, F., et al., 2009. Carbon nanotubes are able to penetrate plant seed coat and dramatically affect seed germination and plant growth. ACS Nano 3, 3221–3227. https://doi.org/10.1021/nn900887m.
Krishnaraj, C., Jagan, E.G., Ramachandran, R., Abirami, S.M., Mohan, N., Kalaichelvan, P.T., 2012. Effect of biologically synthesized silver nanoparticles on *Bacopa monnieri* (Linn.) Wettst. plant growth metabolism. Process Biochem. 47, 651–658.
Kumar, S.P.J., Prasad, S.R., Banerjee, R., Thammineni, C., 2015. Seed birth to death : dual functions of reactive oxygen species in seed physiology. Ann. Bot. 663–668. https://doi.org/10.1093/aob/mcv098.
Lee, W.M., Kwak, J., Il, An, Y.J., 2012. Effect of silver nanoparticles in crop plants *Phaseolus radiatus* and *Sorghum bicolor*: media effect on phytotoxicity. Chemosphere 86, 491–499. https://doi.org/10.1016/j.chemosphere.2011.10.013.
Leymarie, J., Vitkauskaité, G., Hoang, H.H., Gendreau, E., Chazoule, V., Meimoun, P., et al., 2012. Role of reactive oxygen species in the regulation of arabidopsis seed dormancy. Plant Cell Physiol. 53, 96–106. https://doi.org/10.1093/pcp/pcr129.
Liu, R., Lal, R., 2015. Potentials of engineered nanoparticles as fertilizers for increasing agronomic productions. Sci. Total Environ. 514, 131–139. https://doi.org/10.1016/j.scitotenv.2015.01.104.
Lu, W., Senapati, D., Wang, S., Tovmachenko, O., Singh, A.K., Yu, H., et al., 2010. Effect of surface coating on the toxicity of silver nanomaterials on human skin keratinocytes. Chem. Phys. Lett. 487 (1 − 3), 92–96. https://doi.org/10.1016/j.cplett.2010.01.027.
Ma, C., Chhikara, S., Minocha, R., Long, S., Musante, C., White, J.C., et al., 2015. Reduced silver nanoparticle phytotoxicity in *Crambe abyssinica* with enhanced glutathione production by overexpressing bacterial γ-glutamylcysteine synthase. Environ. Sci. Technol. 49 (16), 10117–10126.
Ma, X., Geiser-Lee, J., Deng, Y., Kolmakov, A., 2010. Interactions between engineered nanoparticles (ENPs) and plants: phytotoxicity, uptake and accumulation. Sci. Total Environ. 408 (16), 3053–3061.
Mahakham, W., Theerakulpisut, P., Maensiri, S., Phumying, S., Sarmah, A.K., 2016. Environmentally benign synthesis of phytochemicals-capped gold nanoparticles as nanopriming agent for promoting maize seed germination. Sci. Total Environ. 573, 1089–1102. https://doi.org/10.1016/j.scitotenv.2016.08.120.
Masum, M.M.I., Siddiqa, M.M., Ali, K.A., Zhang, Y., Abdallah, Y., Ibrahim, E., et al., 2019. Biogenic synthesis of silver nanoparticles using *Phyllanthus emblica* fruit extract and its inhibitory action against the pathogen acidovorax oryzae strain RS-2 of rice bacterial brown stripe. Front. Microbiol. 10, 820.
McGillicuddy, E., Murray, I., Kavanagh, S., Morrison, L., Fogarty, A., Cormican, M., et al., 2017. Silver nanoparticles in the environment: sources, detection and ecotoxicology. Sci. Total Environ. 575, 231–246.
Mirzajani, F., Askari, H., Hamzelou, S., Schober, Y., Römpp, A., Ghassempour, A., et al., 2014. Proteomics study of silver nanoparticles toxicity on *Oryza sativa* L. Ecotoxicol. Environ. Saf. 108, 335–339.
Mohanta, Y.K., Panda, S.K., Biswas, K., Tamang, A., Bandyopadhyay, J., De, D., et al., 2016a. Biogenic synthesis of silver nanoparticles from *Cassia fistula* (Linn.): in vitro assessment of their antioxidant, antimicrobial and cytotoxic activities. IET Nanobiotechnol. 10, 438–444. https://doi.org/10.1049/iet-nbt.2015.0104.
Mohanta, Y.K., Singdevsachan, S.K., Parida, U.K., Panda, S.K., Mohanta, T.K., Bae, H., 2016b. Green synthesis and antimicrobial activity of silver nanoparticles using wild medicinal mushroom *Ganoderma applanatum* (Pers.) Pat. from Similipal Biosphere Reserve, Odisha, India. IET Nanobiotechnol. 10 (4), 184–189.
Mohanta, Y.K., Panda, S.K., Jayabalan, R., Sharma, N., Bastia, A.K., Mohanta, T.K., 2017a. Antimicrobial, antioxidant and cytotoxic activity of silver nanoparticles synthesized by leaf extract of *Erythrina suberosa* (Roxb.). Front. Mol. Biosci. 4, 1–14.
Mohanta, Y.K., Biswas, K., Panda, S.K., Bandyopadhyay, J., De, D., Jayabalan, R., et al., 2017b. Phyto-assisted synthesis of bio-functionalised silver nanoparticles and their potential anti-oxidant, anti-microbial and wound healing activities. IET Nanobiotechnol. 11 (8), 1027–1034.
Mohanta, Y.K., Biswas, K., Bandyopadhyay, J., Tamang, A., De, D., Mohanta, D., et al., 2018. *Abutilon indicum* (L.) sweet leaf extracts assisted bio-inspired synthesis of electronically charged silver nano-particles with potential antimicrobial, antioxidant and cytotoxic properties. Mater. Focus 7 (1), 94–100.
Moulton, M.C., Braydich-Stolle, L.K., Nadagouda, M.N., Kunzelman, S., Hussain, S.M., Varma, R.S., 2010. Synthesis, characterization and biocompatibility of "green" synthesized silver nanoparticles using tea polyphenols. Nanoscale 2, 763–770.
Mukherjee, S., Chowdhury, D., Kotcherlakota, R., Patra, S., 2014. Potential theranostics application of bio-synthesized silver nanoparticles (4-in-1 system). Theranostics 4 (3), 316.
Nair, R., 2016. Effects of nanoparticles on plant growth and development. In: Kole, C., Kumar, D.S., Khodakovskaya, M.V. (Eds.), Plant Nanotechnology. Springer International Publishing, Switzerland, pp. 95–118.
Nayak, D., Ashe, S., Rauta, P.R., Kumari, M., Nayak, B., 2016. Bark extract mediated green synthesis of silver nanoparticles: evaluation of antimicrobial activity and antiproliferative response against osteosarcoma. Mater. Sci. Eng. C 58, 44–52. https://doi.org/10.1016/j.msec.2015.08.022.
Nel, A., Xia, T., Madler, L., Li, N., 2006. Toxic potential of materials at the nanolevel. Science 311, 622–627. https://doi.org/10.1126/science.1114397.
Oves, M., Aslam, M., Rauf, M.A., Qayyum, S., Qari, H.A., Khan, M.S., et al., 2018. Antimicrobial and anticancer activities of silver nanoparticles synthesized from the root hair extract of *Phoenix dactylifera*. Mater. Sci. Eng. C 89, 429–443.
Palocci, C., Valletta, A., Chronopoulou, L., Donati, L., Bramosanti, M., Brasili, E., et al., 2017. Endocytic pathways involved in PLGA nanoparticle uptake by grapevine cells and role of cell wall and membrane in size selection. Plant Cell Rep. 36, 1–12.
Pokhrel, L.R., Dubey, B., 2013. Evaluation of developmental responses of two crop plants exposed to silver and zinc oxide nanoparticles. Sci. Total Environ. 452, 321–332. https://doi.org/10.1016/j.scitotenv.2013.02.059.
Ramesh, P.S., Kokila, T., Geetha, D., 2015. Plant mediated green synthesis and antibacterial activity of silver nanoparticles using *Emblica officinalis* fruit extract. Spectrochim. Acta 142, 339–343.
Razack, S.A., Duraiarasan, S., Mani, V., 2016. Biosynthesis of silver nanoparticle and its application in cell wall disruption to release carbohydrate and lipid from *C. vulgaris* for biofuel production. Biotechnol. Rep. 11, 70–76.
Sathishkumar, M., Sneha, K., Won, S.W., Cho, C.W., Kim, S., Yun, Y.S., 2009. *Cinnamon zeylanicum* bark extract and powder mediated green synthesis of nano-crystalline silver particles and its bactericidal activity. Colloids Surfaces B Biointerfaces 73 (2), 332–338.
Scartezzini, P., Antognoni, F., Raggi, M.A., Poli, F., Sabbioni, C., 2006. Vitamin C content and antioxidant activity of the fruit and of the Ayurvedic preparation of *Emblica officinalis* Gaertn. J. Ethnopharmacol. 104, 113–118. https://doi.org/10.1016/j.jep.2005.08.065.
Shalata, A., Neumann, P.M., 2001. Exogenous ascorbic acid (vitamin C) increases resistance to salt stress and reduces lipid peroxidation. J. Exp. Bot. 52 (364), 2207–2211.
Sharma, P., Jha, A.B., Dubey, R.S., Pessarakli, M., 2012. Reactive oxygen species, oxidative damage, and antioxidative defense mechanism in plants under stressful conditions. J. Bot., Le 1–26. https://doi.org/10.1155/2012/217037.
Shaw, A.K., Hossain, Z., 2013. Impact of nano-CuO stress on rice (*Oryza sativa* L.) seedlings. Chemosphere 93 (6), 906–915.
Stampoulis, D., Sinha, S.K., White, J.C., 2009. Assay-dependent phytotoxicity of nanoparticles to plants. Environ. Sci. Technol. 43, 9473–9479. https://doi.org/10.1021/es901695c.
Tamás, L., Šimonovičová, M., Huttová, J., Mistrík, I., 2004. Aluminium stimulated hydrogen peroxide production of germinating barley seeds. Environ. Exp. Bot. 51 (3), 281–288.
Thuesombat, P., Hannongbua, S., Akasit, S., Chadchawan, S., 2014. Effect of silver nanoparticles on rice (*Oryza sativa* L. cv. KDML 105) seed germination and seedling growth. Ecotoxicol. Environ. Saf. 104, 302–309.
Thwala, M., Musee, N., Sikhwivhilu, L., Wepener, V., 2013. The oxidative toxicity of Ag and ZnO nanoparticles towards the aquatic plant *Spirodela punctuta* and the role of testing media parameters. Environ. Sci. Process Impacts 15, 1830–1843. https://doi.org/10.1039/c3em00235g.
Tiquia, S.M., Tam, N.F.Y., Hodgkiss, I.J., 1996. Effects of composting on phytotoxicity of spent pig-manure sawdut litter. Environ. Pollut. 93, 249–256. https://doi.org/10.1016/S0960-8524(97)00080-1.
Tripathi, D.K., Singh, S., Singh, S., Srivastava, P.K., Singh, V.P., Singh, S., et al., 2017. Nitric oxide alleviates silver nanoparticles (AgNps)-induced phytotoxicity in *Pisum sativum* seedlings. Plant Physiol. Biochem. 110, 167–177.
US Department of Agriculture and US Composting Council, 2001. Test methods for the examination of composting and compost. Edaphos Int. Houst.
USEPA, 1996. Ecological effects test guidelines earthworm subchronic toxicity test. United States Environ. Prot. Agency 1–11.
Ushahra, J., Bhati-Kushwaha, H., Malik, C.P., 2014. Biogenic nanoparticle-mediated augmentation of seed germination, growth, and antioxidant level of *Eruca sativa* mill. varieties. Appl. Biochem. Biotechnol. 174 (2), 729–738.
Vannini, C., Domingo, G., Onelli, E., De, Mattia, F., Bruni, I., Marsoni, M., et al., 2014. Phytotoxic and genotoxic effects of silver nanoparticles exposure on germinating wheat seedlings. J. Plant Physiol. 171, 1142–1148. https://doi.org/10.1016/j.jplph.2014.05.002.
Vannini, C., Domingo, G., Onelli, E., Prinsi, B., Marsoni, M., Espen, L., et al., 2013. Morphological and proteomic responses of *Eruca sativa* exposed to silver nanoparticles or silver nitrate. PLoS One 8 (7), e68752. https://doi.org/10.1371/journal.pone.0068752.
Vijayakumar, M., Priyam, K., Nancy, F.T., Noorlidah, A., Ahmed, A.B.A., 2013. Biosynthesis, characterisation and anti-bacterial effect of plant-mediated silver nanoparticles using Artemisia nilagirica. Ind. Crops Prod. 41, 235–240.

Walker, G.W., Kookana, R.S., Smith, N.E., Kah, M., Doolette, C.L., Reeves, P.T., et al., 2017. Ecological risk assessment of nano-enabled pesticides: a perspective on problem formulation. J. Agric. Food Chem. 66 (26), 6480–6486.

Wang, Y.H., Zhang, G., Chen, Y., Gao, J., Sun, Y.R., Sun, M.F., et al., 2019. Exogenous application of gibberellic acid and ascorbic acid improved tolerance of okra seedlings to NaCl stress. Acta Physiol. Plant. 41 (6), 93.

Wang, Z., Li, J., Zhao, J., Xing, B., 2011. Toxicity and internalization of CuO nanoparticles to prokaryotic alga *Microcystis aeruginosa* as affected by dissolved organic matter. Environ. Sci. Technol. 45 (14), 6032–6040.

Wojtyla, L., Lechowska, K., Kubala, S., Garnczarska, M., 2016. Different modes of hydrogen peroxide action during seed germination. Front. Plant Sci. 7, 1–16. https://doi.org/10.3389/fpls.2016.00066.

Xiong, J., Wang, Y., Xue, Q., Wu, X., 2011. Synthesis of highly stable dispersions of nanosized copper particles using L -ascorbic acid. Green Chem. 13 (4), 900–904. https://doi.org/10.1039/c0gc00772b.

Xu, Q.S., Hu, J.Z., Xie, K.B., Yang, H.Y., Du, K.H., Shi, G.X., 2010. Accumulation and acute toxicity of silver in *Potamogeton crispus* L. J. Hazard Mater. 173, 186–193.

Yasur, J., Rani, P.U., 2013. Environmental effects of nanosilver: impact on castor seed germination, seedling growth, and plant physiology. Environ. Sci. Pollut. Res. 20, 8636–8648. https://doi.org/10.1007/s11356-013-1798-3.

Zahran, M.K., Ahmed, H.B., El-Rafie, M.H., 2014. Alginate mediate for synthesis controllable sized AgNPs. Carbohydr. Polym. 111, 10–17. https://doi.org/10.1016/j.carbpol.2014.03.029.